Iranian Journal of Catalysis 8(2), 2018, 95-102

IRANIAN JOURNAL OF CATALYSIS

Magnetically separable $MgFe_2O_4$ nanoparticle for efficient catalytic ozonation of organic pollutants

Akbar Eslami[a], Ali Oghazyan[b], Mansour Sarafraz[c,*]

[a]*Environmental and Occupational Hazards Control Research Center, Shahid Beheshti University of Medical Sciences, Tehran, Iran.*

[b]*Department of Environmental Health Engineering, School of Public Health, Shahid Beheshti University of Medical Sciences, Tehran, Iran.*

[c]*Student Research committee, School of Public Health, Shahid Beheshti University of Medical Sciences, Tehran, Iran.*

Received 23 July 2017; received in revised form 29 January 2018; accepted 1 February 2018

ABSTRACT

Magnetically separable $MgFe_2O_4$ was synthesized and used in catalytical ozonation of 4-chlorophenol (4-CP). The prepared catalyst was characterized by X-Ray Diffraction (XRD), Field Emission Scanning Electronic Microscopy (FE-SEM), Transmission Electron Microscopy (TEM), Brunauer−Emmett−Teller (BET) and Vibrating-Sample Magnetometer (VSM). The optimum conditions for the highest efficacy of the catalytic ozonation process were found to be pH 7, catalyst dose 0.2 g/L, O_3 concentration 1.67 mg/L.min, contact time of 30 min and 4-CP concentration 100 mg/L. At these optimal conditions, the efficiency of process was 93.5%. In addition, the results showed that the catalyst can significantly enhance the mineralization of 4-CP, and more than 70% 4-CP were mineralized in the presence of the catalyst, that is almost 2.5 times higher than ozonation alone. Moreover, the results revealed that the removal efficiency was not affected by solution pH and removal efficiency in the $O_3/MgFe_2O_4$ process exceeded 90% over a wide pH range of 4–10. This study demonstrates that $MgFe_2O_4$ is a recyclable and efficient catalyst in the ozonation organic pollutants.

***Keywords**: Catalytic ozonation, Mineralization, Magnesium ferrite, 4-Chlorophenol, Sol-gel.*

1. Introduction

Water polluted with organic contaminants is a serious environmental challenge [1]. Refractory organic compounds are highly toxic and slowly biodegradable so they can cause significant damage to natural water systems and human health. Removing these contaminants using conventional treatment such as adsorption, biological degradation, or chemical oxidation, is not effective [2]. In the current decade, advanced oxidation processes (AOPs) have been recommended as an effective and emerging option for the treatment of wastewater containing persistent organic compounds [3]. Among these AOPs methods, the catalytic ozonation process, because of its ability to degrade and mineralize these types of contaminants, has attracted the most attention.

*Corresponding author email: mansour.sarafraz@yahoo.com
Tel.: +98 21 2243 9982; Fax: +98 21 2243 9784

Catalysts improve the ozone decomposition and produce highly active radical species, especially the hydroxyl radical ($^{\bullet}OH$) [4]. This process is highly efficient and its operational conditions show great potential for use at fullscale wastewater treatment plants without adding any additional tools [5]. Typically, metal oxides such as MnO_2 [6] and MgO [7]; coated metal oxides, including CeO_2/Al_2O_3 or SiO_2 or TiO_2 [8], along with some porous compounds such as mesoporous carbon [9] are suggested as the catalysts for ozonation. Chen et al. investigated the catalytic performance of MgO with different exposed crystal facets towards the ozonation of 4-chlorophenol; results showed that the catalytic ozonation on each MgO substantially enhanced the removal of 4-chlorophenol and total organic carbon, compared with ozonation alone or that on traditional MgO [10]. In another study catalytic activities of ultra-small β-FeOOH nanorods were examined for ozonation of 4-chlorophenol. The removal efficiency of 4-CP was

significantly enhanced in the presence of β-FeOOH compared to ozone alone[11]. However, these catalysts are typically used in micro- or nano-size powder, and it is difficult to separate them from treated water. Nano-magnetic compounds solve this problem because they are insoluble and have a paramagnetic nature; this enables easy and effective separation of the reaction mixture using an external magnet [12]. Because of its attractive magnetic and electrical properties with chemical and thermal stabilities, spinel ferrites with the general formula $MeFe_2O_4$ (Me = Mg, Ni, Ca, or Zn) are applied as main magnetic materials [13]. Magnesium ferrite ($MgFe_2O_4$) is one of the most important magnetic oxides with a spinel structure [14]. This environmentally friendly compound has unique characteristics, including high surface activity and reactivity, high stability in water, and low toxicity [15]. Therefore, it is reasonable to believe that this compound may show a high catalytic activity. In this study, we selected the 4-chlorophenol as the target contaminant. This compound is one of the most important organic contaminants in industrial wastewaters and also widely identified in water and wastewater[16]. Because of acute toxicity and resistance to biological degradation, chlorophenols are in the group of persistent organic pollutants (POPs) [17]. 4-chlorophenol (4-CP) is widely produced as a by-product of certain industrial processes, including the production of rubber, resins, textiles, steel, paper, and in petrochemical industries [18]. The aim of this study is the synthesis and characterization of $MgFe_2O_4$ and comparison of ozonation and the catalytic ozonation process with $MgFe_2O_4$ for removal of 4-chlorophenol.

2. **Experimental**

2.1. Materials and reagents

Magnesium nitrate hexahydrate ($Mg(NO_3)_2.6H_2O$, Merck) and Iron (III) nitrate nonahydrate ($Fe(NO_3)_3.9H_2O$, Merck) were used as precursors. 4-Chlorophenol analytical grade (98.0%) was used as a model compound in the experiment and purchased from Merck. 4-aminoantipyrine (AAP) and potassium ferricyanide were purchased from Sigma-Aldrich. All reagents used in the experiment were of analytical reagent grade and used without further purification.

2.2. Catalyst preparation

To prepare $MgFe_2O_4$, a sol-gel combustion process was employed [19]. Briefly, $Mg(NO_3)_2{\cdot}6H_2O$ and $Fe(NO_3)_3{\cdot}9H_2O$ were dissolved into distilled water with a stoichiometric ratio of Mg:Fe=1:2. Afterward, to yield a citrate–nitrite ratio of 1.0, citric acid was added drop-wise to the solution as fuel. The solution pH was adjusted to 5 by a concentrated ammonium solution and the resulting solution was evaporated at 80 °C to achieve a solid-liquid phase compound under continuous stirring conditions. The obtained compound was directly transferred to a muffle furnace; the temperature was then increased gradually up to 450 °C and was kept at this temperature for 2 hours; finally, the branch-like foam was crushed and passed through a 200-mesh sieve and then stored in a desiccator for use in the experiments.

2.3. Experimental procedure

Catalytic ozonation experiments were carried out in a semi-batch mode by continuously feeding ozone gas to a plexiglass reactor. For each experiment, 2 L of simulated wastewater containing 100 mgL^{-1} of 4-CP and a certain amount of catalyst powder were added in to the reactor. Ozone was generated using a laboratory ozone generator (SS4, shamimsharif co, Iran) with 20 g O_3 h^{-1} capacity. The ozonation was started at the dosage of 1.67 mg/min and continued for the desired time period (5-30 min). The excess ozone in the outlet gas was trapped by a KI solution. Finally, after filtration of effluent sample through 0.22 µm millipore membrane filters to remove suspended particles, the samples were instantly analyzed. All experiments were performed at an average ambient temperature of 23 ± 2°C. Fig. 1 shows a schematic of the experimental set-up used for the ozonation experiments.

2.4. Analytical method

Transmission electron micrographs were obtained using an EM10C (Germany) microscope operating at accelerating voltage of 80 kV. Specific surface area, volume, and size of pores were measured using nitrogen adsorption–desorption at 77 K using a Belsorp mini II (Japan) and calculated according to the Brunauer−Emmett−Teller (BET) and Barrett–Joyner–Hanlenda (BJH) isotherm models. The pore volume and the average pore size of the samples were determined at a relative pressure (P/P0) of 0.986, based on volume of adsorbed nitrogen. The pH_{pzc} was determined based on the batch equilibration technique [20]. Magnetic properties were evaluated at room temperature with a magnetic property measurement system (BDKFD-Meghnatis kavir- Iran). The concentration of 4-CP was analyzed by a UV–vis spectrophotometer (DR-5000, HACH LANGE, USA) with absorption at 500 nm using the colorimetric method of 4-aminoantipyrine with $K_3Fe(CN)_6$ in a NH_4Cl/NH_3 buffer solution. Chloride ions were determined with the argentometric method of titration with silver nitrate.

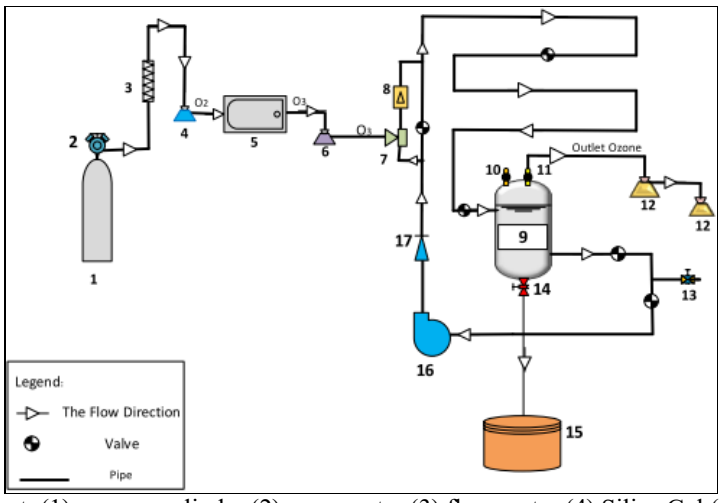

Fig. 1. Experimental equipment: (1) oxygen cylinder (2) manometer (3) flow meter (4) Silica Gel (5) ozone generator stirrer; (6) water trap (7) venturi (8) check valve (9) reactor; (10) inlet valve (11) air valve (12) KI trap (13) sampling valve (14) outlet valve (15) effluent disposal (16) centrifuge pump (17) pressure reducing valve.

The total organic carbon (TOC) was measured by a TOC analyzer (Shimadzu, Japan). X-ray diffraction patterns of the samples were carried out at room temperature by a STOE (Theta-Theta, Germany) diffractometer using Cu Kα radiation (λ =1.54060å). Generator settings were 40 kV, 40 mA. Data were obtained in the 2θ range 10–80°. The average dimension (D) of particles was estimated by the Debye–Scherrer's formula[21], based on widening of the anatase (101) peak as:

$$D = \frac{k\lambda}{\beta \cos\theta}$$

Where λ is the X-ray wavelength of the Cu Kα radiation (nm), β is the peak width of the diffraction peak profile at half maximum height resulting from the small crystallite size (radians), and K is a coefficient relating to crystallite shape which is normally equal to 0.9.

3. Results and Discussion

3.1. Catalysts characterization

Fig. 2 shows the XRD pattern, TEM and FESEM image, VSM and BET curve of prepared catalyst. To determine the structure and phase of $MgFe_2O_4$ nanoparticles, XRD pattern were investigated and is shown in Fig. 2(a). The observed peak position and relative intensity of all diffraction peaks were coordinated well with standard powder diffraction data (ICSD 01-071-1232). The diffraction peaks at 2θ = 30.15°, 35.5°, 43.1°, 53.6°, 57°, and 62.6° can be ascribed to Bragg reflections of (220), (311), (400), (422), (511) and (440) planes which can be readily indexed to the spinel phase. Furthermore, lack of any impure peak in these patterns suggests that a pure cubic $MgFe_2O_4$ nanoparticle is formed.

The XRD pattern represents the crystal phase of $MgFe_2O_4$ with a spinel structure in the combustion process. According to the Debye– Scherrer formula, the average crystallite size can be estimated from the half-width of the most intense peak (311). The size of the crystals layer was estimated 33 nm using the Scherrer equation, suggesting achievement to nanoscale crystals. The Field Emission Scanning Electron Microscopy (FESEM) test was used to understand the morphology and surface structure of the $MgFe_2O_4$ nanoparticles. Fig. 2(b) displays the dense and cumulative structure of the $MgFe_2O_4$ nanoparticles. Furthermore, with close observation we can see the presence of particles in the cubic phase. To specifically investigate the distribution of the size of the nanoparticles, a TEM image was taken from the sample. As shown in Fig. 2(c), the distribution of the particles is in the form of cubic spinel and not uniform. Besides, the size of the particles is below 100 nm;this confirms the size obtained by the Scherer equation. Fig. 2(d) shows the adsorption/desorption isotherm of the nitrogen of $MgFe_2O_4$ nanoparticles and the size distribution of the pores of these nanoparticles. As displayed this isotherm follows isotherm Type IV. Moreover, the pore size distribution of $MgFe_2O_4$ below 61 nm was obtained, mainly between 2 and 30 nm with peak of 2.4 nm. The BET surface area and the total volume of the pores are 98 $m^2\ g^{-1}$ and 0.32 $cm^3\ g^{-1}$, respectively. $MgFe_2O_4$ prepared by a sol–gel method shows high S_{BET} because large gaseous materials were produced during the auto-combustion process and acted as pore-fabricating agents[22]. The vibrating-sample magnetometer (VSM) technique was applied to evaluate the magnetic properties of $MgFe_2O_4$. The hysteresis loop traced at room temperature for $MgFe_2O_4$ is shown in Fig. 2(e).

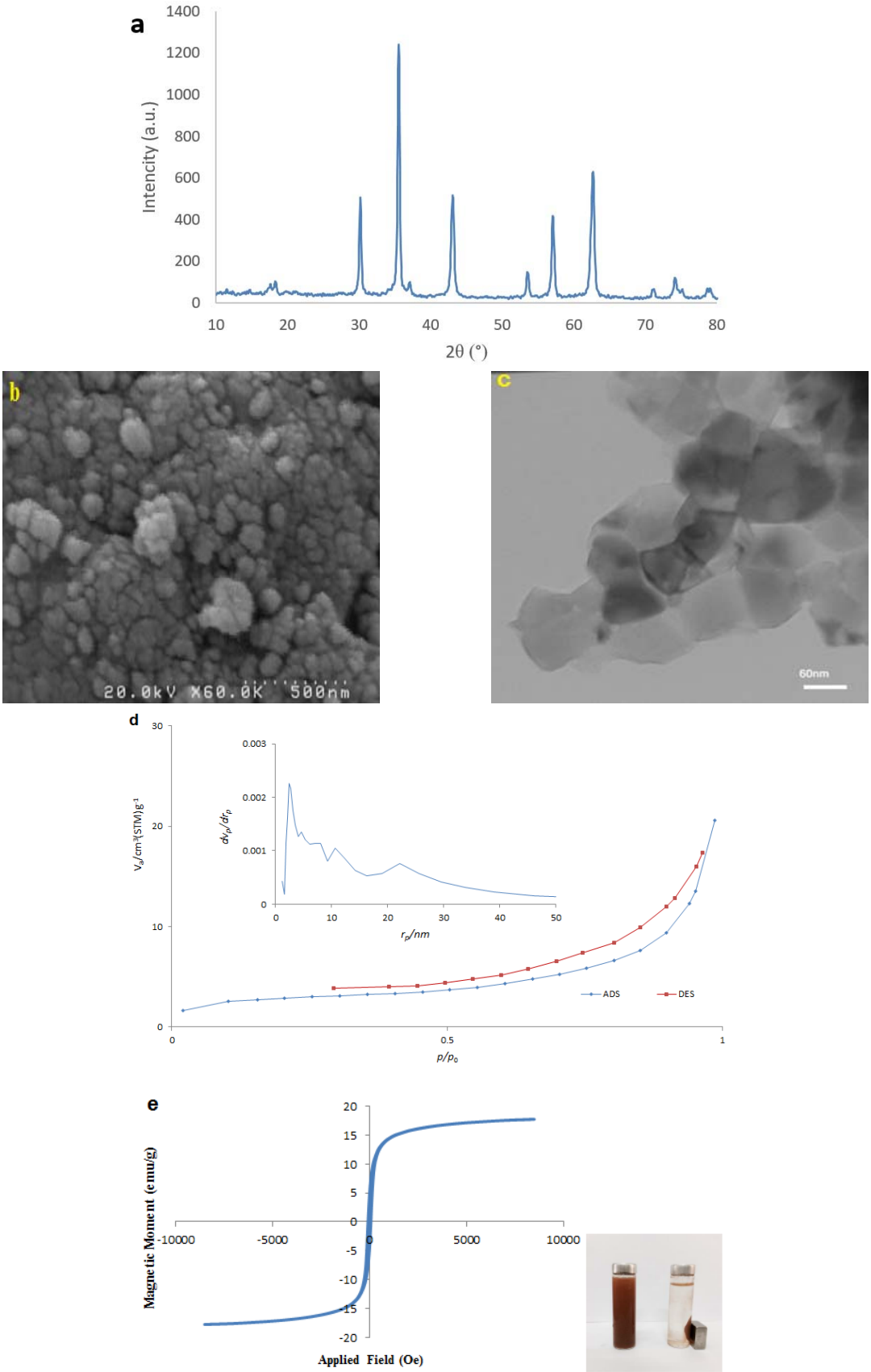

Fig. 2. Characterization of $MgFe_2O_4$: (a) XRD pattern; (b) FESEM image; (c) TEM image; (d) N_2 adsorption/desorption isotherm and pore size distribution; and (e) magnetic hysteresis loops at room temperature.

The hysteresis loop explains the soft magnetic nature of the synthesized $MgFe_2O_4$ and also the large saturation magnetization (Ms) of 17.7 $emug^{-1}$. $MgFe_2O_4$ particles can simply be recovered from the reaction solution by using an external magnetic field. Highly efficient recyclability is economically suitable for practical applications.

3.2. Comparison of ozonation alone and catalytic ozonation with $MgFe_2O_4$

Catalytic activity of $MgFe_2O_4$ for the degradation of 4-CP in aqueous solution was studied at three different processes namely ozonation alone (O_3); catalytic ozonation using $MgFe_2O_4$ nanoparticles ($O_3/MgFe_2O_4$) and adsorption on $MgFe_2O_4$ nanoparticles. To evaluate the 4-CP adsorption on the surface of the catalyst, an adsorption experiment was conducted under similar conditions with the experimental conditions used in the catalytic activity experiment, but in the absence of ozone. As observed in Fig. 3, the adsorption process on $MgFe_2O_4$ nanoparticles showed an efficiency of 25% after 30 min. The good adsorption capability of $MgFe_2O_4$ is probably due to the electrostatic attraction between 4-CP and $MgFe_2O_4$ at pH 5.5. On the other hand, as shown in Fig. 4(b), the pH_{PZC} of $MgFe_2O_4$ was 9.8, which is much higher than the solution pH of 5.5. Therefore, the surface of $MgFe_2O_4$ particles would be significantly positively charged and thus attract the 4-CP anions.

As shown in Fig. 3, ozonation process enhanced the removal of 4-CP compared with adsorption of 4-CP However, the best result was obtained for the $O_3/MgFe_2O_4$ process. At the end of the reaction (30 min), the efficiency of the combinational process of $O_3/MgFe_2O_4$ is 92.6%. When $MgFe_2O_4$ was added, the degradation of 4-CP may increase due to a combination of adsorption and/or reaction with radical species (e.g.,$^{\bullet}OH$) produced as a result of ozone decomposition in the presence of $MgFe_2O_4$. The ozone decomposition mechanisms onto metal oxide surfaces are shown in Scheme (1) and (2).[23] The lower electronegativity or the higher metallicity of Mg leads to the higher electron density of O^{2-} and Mg bond, and consequently results in the catalytic decomposition of ozone into radicals due to the electrophilic property of ozone molecules [24]:

$$\equiv OM + O_3 \rightarrow \equiv OM - O - O - O^{\bullet} \quad (1)$$

$$\equiv OM - O - O - O^{\bullet} \rightarrow O_2 + \equiv OM - O^{\bullet} \quad (2)$$

In fact, $MgFe_2O_4$ catalyst might accelerate the decomposition of O_3 molecules to hydroxyl radicals ($^{\bullet}OH$), which could enhance the oxidizing activity of the process [15,19].

3.3. Effect of pH and catalyst dosage

Since the initial pH of the solution is one of the major influential factors in production of hydroxyl radical from O_3 decomposition, ozonation experiments were performed under different initial pHs (4, 5.5, 7, 8.5 and 10). In Fig. 4 (a), the effect of initial pH on the 4-CP degradation efficiency is shown in two processes including O_3 and $O_3/MgFe_2O_4$. Surprisingly neither process was not affected by changing initial pH. Based on previous studies, the catalytic ozonation process is usually dependent on pH. For example, Qi et al investigated catalytic ozonation of 4-CP using a $MnO_x/\gamma\text{-}Al_2O_3/TiO_2$ catalyst. The process was also highly dependent on pH, which increased from 2.57 to 11.13; 4-CP degradation efficiency increased from 59.59 to 99.77% [18].

Moreover, solution pH which is one of the important parameters, determines catalyst surface charge, dissolving of semiconductors in the suspension and ionic forms of pollutant present in the suspension[26].

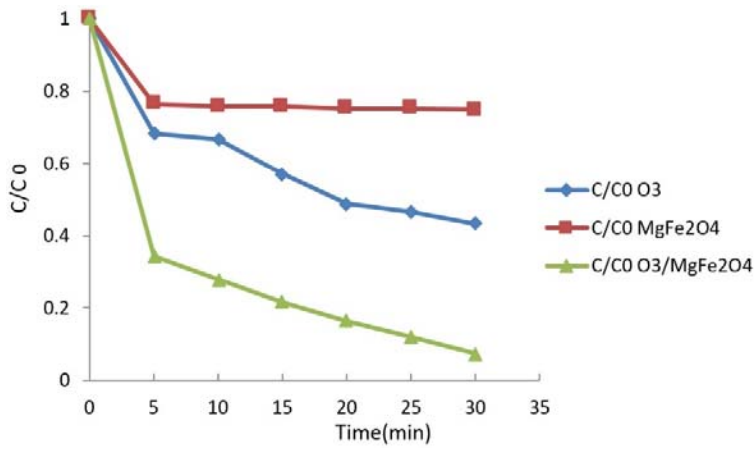

Fig. 3. Comparison of 4-CP removal in the O_3, adsorption by $MgFe_2O_4$ and $O_3/MgFe_2O_4$ processes in different reaction time. (ozone gas concentration, 1.67 mg/L; initial concentration of 4-CP, 100 mg/L; catalyst dosage = 0.2 g/L, pH= 7).

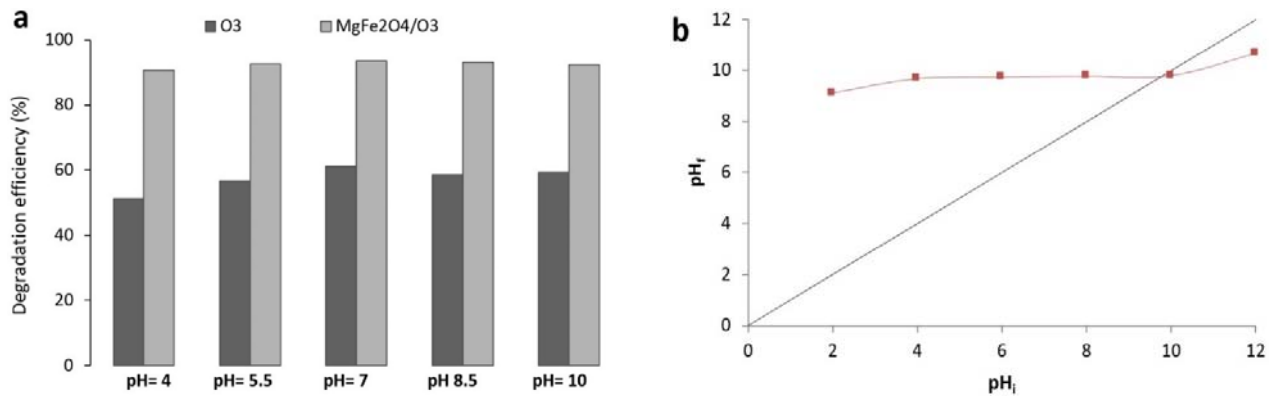

Fig. 4. Effect of pH on 4-CP degradation. (a) zero point charge of 4-CP (b) degradation efficiency of 4-CP in the O_3 and O_3/ $MgFe_2O_4$ processes (ozone gas concentration, 1.67 mg/L; initial concentration of 4-CP, 100 mg/L; catalyst dosage = 0.2 g/L)

Therefore, the reason for the suitable performance of the process was studied in this research and its independence from pH can be related to the hydroxyl functional group of 4-CP (with a pK_a=9.4), which is a type of weak acid that becomes ionized in environments with a pH below 9.4 and will have a negative charge. Good degradation rate in the alkaline medium may be attributed to more hydroxide ions (OH^-) in the solution producing more hydroxyl radicals ($OH^•$). Since hydroxyl radical is the dominant oxidizing species in the catalytic ozonation process, the degradation of 4-CP is therefore accelerated in an alkaline medium. The reason for the increase of degradation rate at low initial pH value is because of more H^+ ions in the solution; more conduction band electrons (e^-) can transfer to the surface of catalyst to react with O_2 to produce more hydroxyl radicals[27]. Besides, the catalyst surface will be charged negatively when pH> pH_{zpc}, positively when pH< pH_{zpc} and neutrally when pH ≈ pH_{zpc}. Fig. 4(b) shows the zero point charge of the prepared nanoparticle-$MgFe_2O_4$. As shown in the figure, pH of the zero point charge (pH_{zpc}) was determined to be 9.8, thus at a pH below 9.8, the surface of the absorbent will have a positive charge and can absorb negatively charged chlorophenol molecules. In addition, this increase in the rate of degradation can be due to adsorption and reaction with the obtained radical species, especially the hydroxyl radical from ozone decomposition on the surface of $MgFe_2O_4$. Finally, due to independence of the process from the initial pH, the neutral pH (pH=7) was chosen as the optimum pH and used for further experiments.

The catalyst dose which is an important parameter in the heterogeneous catalytic ozonation process, is effective in the conversion of ozone to radical species and influences adsorption of the dissolved substance [25]. Therefore, investigation of the effect of the catalyst dose on the degradation efficiency and finding the optimum dose will be essential for this process. In this study, the effect of the catalyst dose on 4-CP removal was studied within the range of 0.1-0.5 g/l. As can be seen in Fig. 5, by increasing the catalyst dose from zero to 0.2 g/l, 4-CP degradation efficiency rises from 61.2% to 93.5%, and with a further increase up to 0.5 g/l: no significant development occurs in the degradation efficiency (degradation efficiency=93.6%). Although $MgFe_2O_4$ made it possible that the chain of radical reactions could be induced and propagated by the ozone introduced in the reactor, the excess $MgFe_2O_4$ particles easily aggregated and affected the use efficiency [28]. Therefore, a dose of 0.2 g/l was chosen as the optimum dose to be used in other experiments.

3.4. Mineralization and dechlorination of 4-CP

When AOPs technologies were applied to degradation, after determining the contributors to 4-CP degradation; the formation and accumulation of chloride ions as the major inorganic product in the degradation of 4-CP by catalytic ozonation process, can be attractive. Therefore, the ‘‘dechlorination efficiency’’ is defined as the transformation process in 4-CP, that was degraded and converted to chloride ions. To this purpose, experiment of dechlorination was done for influent synthetic wastewater and optimum condition was selected for degradation of 4-CP. Under this condition, the rate of dechlorination was obtained to be 86.8%. Researchers proved that biodegradation processes have the high potential for biodegradability and free toxicity of organic compounds [29]. Also, rate of TOC removal was measured in order to investigate the mineralization degree. TOC removal efficiency was obtained to be 28.55 and 71% for O_3 and the O_3/$MgFe_2O_4$ process after 30 min, respectively. It was also observed that in the O_3/$MgFe_2O_4$ process, with the increase in the experimental time to 1 hour, TOC removal efficiency did not change significantly (75%).

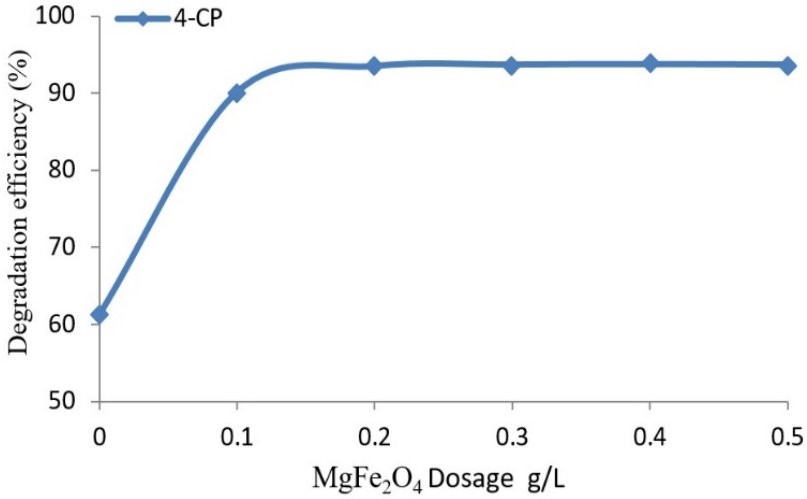

Fig. 5. Effect of $MgFe_2O_4$ dose on the removal of 4-CP. Conditions: ozone gas concentration, 1.67 mg/L; initial concentration of 4-CP, 100 mg/L; pH: 7.

The aforementioned results suggest a positive effect of the $O_3/MgFe_2O_4$ process on the mineralization of 4-CP compared with ozonation alone (the removal efficiency of $O_3/MgFe_2O_4$ was 2.5 times of ozonation alone). The reason for this increase in the efficiency of TOC removal can be attributed to catalytic decomposition of O_3 to $^{\bullet}OH$ which improved 4-CP mineralization rate [30]. According to results, it is essential to mention that $^{\bullet}OH$ produced from the catalytic ozonation process has sufficient capability to mineralize and cleave of C-Cl bound; this can reduce toxicity of 4-CP and increase biodegradability, both of which can be benefit for biodegradation processes [29].

4. Conclusions

Magnetically separable mesoporous $MgFe_2O_4$ was successfully prepared by a sol–gel combustion method and used as a new ozonation catalyst. The catalytic activity of this nanoparticle was evaluated through ozonation of 4-CP. In the $O_3/MgFe_2O_4$ process, 4-CP removal efficiency within 30 min was 93.5%. Under same conditions, TOC removal efficiency and the rate of dechlorination were 71% and 86.6%, respectively. However, in ozonation process alone, the 4-CP and TOC removal efficiencies were 61.2% and 28.55%, respectively. The independence of the $O_3/MgFe_2O_4$ process from pH allows for usage of this process in the treatment of pH-variable wastewater. Moreover, $MgFe_2O_4$ nanocatalysts could be easily and efficiently separated from the reaction mixture with an external magnet; this made it an attractive nanomaterial with prospective application in catalytic ozonation of organic pollutants in wastewater treatment.

Acknowledgements

The authors are grateful to the Department of Environmental Health Engineering, Shahid Beheshti University of Medical Sciences, Tehran, Iran, for its financial support to and collaboration in this research.

References

[1] S. Xing, X. Lu, J. Liu, L. Zhu, Z. Ma, Y. Wu, Chemosphere 144 (2016) 7-12.
[2] T. Yamamoto, S.I. Kim, J. Chaichanawong, E. Apiluck, T. Ohmori, Appl. Catal. B 88 (2009) 455–461.
[3] M. Sarafraz, M. Khosravi, Gh. Bonyadinejad, A. Ebrahimi, S.M. Taghavi-shahri, Int. J. Environ. Health Eng. 4 (2015) 2-8.
[4] J. Wu, L. Ma, Y. Chen, Y. Cheng, Y. Liu, X. Zha, Water Res. 92 (2016) 140–148.
[5] E. Hu, X. Wu, S. Shang, X.M. Tao, S.X. Jiang, L. Gan, J. Clean. Prod. 112 (2016) 4710–4718.
[6] S.P. Tong, W.P. Liu, W.H. Leng, Q.Q. Zhang, Chemosphere 50 (2003) 1359–1364.
[7] G. Moussavi, M. Mahmoudi, Chem. Eng. J. 152 (2009) 1–7.
[8] S. Maddila, V.D.B.C. Dasireddy, S.B. Jonnalagadda, Appl. Catal. B 138–139 (2013) 149–160.
[9] C.A. Orge, J.P.S. Sousa, F. Gonçalves, C. Freire, J.J.M. Órfão, M.F.R. Pereira, Catal. Lett. 132 (2009) 1–9.
[10] J. Chen, S. Tian, J. Lu, Y. Xiong, Appl. Catal. A 506 (2015) 118–125.
[11] O. Oputu, M. Chowdhury, K. Nyamayaro, O. Fatoki, V. Fester, J. Environ. Sci. 35 (2015) 83–90.
[12] H. Zhao, Y. Dong, G. Wang, P. Jiang, J. Zhang, L. Wu, K. Li, Chem. Eng. J. 219 (2013) 295–302.
[13] M. Li, H.Y. Bai, Z.L. Da, X. Yan, C. Chen, J.H. Jiang, W.Q. Fan, W.D. Shi, Cryst. Res. Technol. 249 (2015) 244–249.

[14] S.M. Hoque, M. Abdul Hakim, Al. Mamun, S. Akhter, Md. Tanvir Hasan, D. Prasad Paul, K. Chattopadhayay, Mater. Sci. Appl. 2 (2011) 1564–1571.
[15] A. Mashayekh-Salehi, G. Moussavi, K. Yaghmaeian, Chem. Eng. J. 310 (2017) 157–169.
[16] A. Nezamzadeh-Ejhieh Z. Ghanbari-Mobarakeh, J. Ind. Eng. Chem. 21 (2014) 668-676.
[17] J. Zhao, X. Chen, L. Bao, Z. Bao, Y. He, Y. Zhang, J. Li, Chemosphere 153 (2016) 138–145.
[18] L. Qi, H. You, Z. Zhang, C. Feng, S. Van Agtmaal, Int. J. Electrochem. Sci. 8 (2013) 5457–5468.
[19] J. Lu, X. Wei, Y. Chang, S. Tian, Y. Xiong, J. Chem. Technol. Biotechnol. 91 (2016) 985–993.
[20] A. Eslami, M.M. Amini, A.R. Yazdanbakhsh, A. Mohseni-Bandpei, A.A. Safari, A. Asadi, J. Chem. Technol. Biotechnol. 91 (2016) 2693–2704.
[21] M. Bordbar, S. Forghani-Pilerood, A. Yeganeh-Faal, Iran. J. Catal. 6 (2016) 415–421.
[22] L. Kong, Y. Xiong, S. Tian, R. Luo, C. He, H. Huang, Bioresour. Technol. 146 (2013) 457–462.
[23] B. Acedo, O. Gimeno, F.J. Rivas, M. Carbajo, F.J. Beltra, Appl. Catal. B 62 (2006) 93–103.
[24] H. Jung, H. Park, J. Kim, J.-H. Lee, H.-G. Hur, N.V. Myung, H. Choi, Environ. Sci. Technol. 41 (2007) 4741–4747.
[25] C. Tizaoui, H. Mohammad-Salim, J. Suhartono, Ozone Sci. Eng. 37 (2015) 269–278.
[26] N. Ajoudanian A. Nezamzadeh-Ejhieh, Mater. Sci. Semicond. Process 36 (2015) 162–169.
[27] Z. Ai, P. Yang, X. Lu, J. Hazard. Mater. 124 (2005) 147–152.
[28] J. Chen, W. Wen, L. Kong, S. Tian, F. Ding, Y. Xiong, Ind. Eng. Chem. Res. 53 (2014) 6297-6306.
[29] A. Yazdanbakhsh, A. Eslami, G. Moussavi, M. Rafiee, A. Sheikhmohammadi, Chemosphere 191 (2018) 156–165.
[30] B. Kasprzyk-Hordern, M. Ziółek, J. Nawrocki, Appl. Catal. B 46 (2003) 639–669.